On the origin of carbon supersaturation in bainitic ferrite

Imed-Eddine Benrabah, Yves Brechet, Christopher Hutchinson, Hatem Zurob

Scripta Materialia 250 (2024) 116182

Contents lists available at ScienceDirect

Scripta Materialia

journal homepage: www.journals.elsevier.com/scripta-materialia

On the origin of carbon supersaturation in bainitic ferrite

Imed-Eddine Benrabah [a,b,*], Yves Brechet [c], Christopher Hutchinson [c,1], Hatem Zurob [b]

[a] Université de Lorraine, CNRS, IJL, F-54000 Nancy, France
[b] Department of Materials Science and Engineering, McMaster University, 1280 Main Street West, Hamilton, ON L8S4L7, Canada
[c] Department of Materials Science and Engineering, Monash University, Clayton, VIC 3800, Australia

ARTICLE INFO

Keywords:
Bainite
Supersaturation
Zener-hillert
Lengthening kinetics

ABSTRACT

Growing evidence in the literature highlights the presence of bainitic ferrite with partial carbon supersaturation at low temperatures. Diffusional growth models correctly predict the lengthening rate of plate-like ferrite but often underestimate carbon content due to the assumption of carbon local equilibrium at the interface, valid at elevated temperatures but less so as temperature decreases. Carbon transfer across the interface becomes increasingly important during bainite formation at lower temperatures, potentially resulting in carbon supersaturation within ferrite. This study proposes a more realistic approach for the carbon interfacial conditions. By relaxing the local equilibrium assumption, a potential carbon activity difference arises between austenite and growing bainite, inducing carbon supersaturation. Comparative analysis with literature data demonstrates that the revised Zener-Hillert model can predict carbon supersaturation trends across diverse alloys and temperatures. This extended model enhances our understanding of bainite growth at lower temperatures, with implications for alloy design and heat treatment processes.

The mechanism of the bainite transformation has long attracted attention from researchers due to the theoretical complexity of the problem and the significant industrial applications of bainite containing steels. Scientific debate persists around two apparently distinct theories to describe the growth kinetics of bainite [1–14]. The key difference between the two theories is the question of whether the carbon is rejected from bainitic ferrite into austenite as the interface migrates, or after [1,6]. In the diffusionless theory, bainitic ferrite inherits the carbon content of the parent austenite during growth, and the freshly formed bainite would be supersaturated with carbon [4,5]. Carbon partitioning is presumed post-bainitic transformation. On the other hand, the diffusional theory assumes that carbon partitioning occurs during the transformation. In this approach, carbon diffusion partially controls the velocity of the interface and the fresh bainite is formed with an "local equilibrium" carbon content [9,13]. The diffusional calculations usually employ the "para-equilibrium" (PE) concept, which significantly modifies the carbon content of austenite, but has little impact on the supersaturation in ferrite. Over several decades, the question of carbon supersaturation within bainitic ferrite has attracted the attention of physical metallurgists.

The Zener-Hillert diffusional theory has often been used to describe the growth kinetics of plate-like ferrite, including bainite [13,15–17]. This theory assumes that carbon diffusion within austenite away from the migrating interface controls the bainite growth kinetics. Two criticisms can be raised against this model. First, experimentally measured bainite growth kinetics were often observed to be slower than those calculated using the original Zener-Hillert theory [10,13,18]. Addressing this, Hillert [11] and, more recently, Leach et al. [13] proposed the existence of a 'barrier' force which slows down the growth of bainite. The magnitude of the barrier is usually adjusted to fit the experimental data. Recently, the present authors have proposed a physically based explanation for this barrier energy, attributing it to the interaction between the advancing interface and existing defects within the matrix, which hinders bainite plate growth, and have shown that this modification to the Zener-Hillert model can describe well the growth kinetics observed experimentally [19].

At elevated temperatures, high carbon diffusivity supports the assumption of local equilibrium across the migrating interface, and this assumption appears well justified, e.g. [20,21]. However, as the reaction temperature is lowered, within the bainite-forming regime, and where

* Corresponding author at: Université de Lorraine, CNRS, IJL, F-54000 Nancy, France.
E-mail address: imed-eddine.benrabah@univ-lorraine.fr (I.-E. Benrabah).

[1] Christopher Hutchinson was an Editor of the journal during the review period of the article. To avoid a conflict of interest, Christopher Hutchinson was blinded to the record and another editor processed this manuscript.

https://doi.org/10.1016/j.scriptamat.2024.116182
Received 31 January 2024; Received in revised form 11 May 2024; Accepted 15 May 2024

carbon diffusion is much slower, the validity of the local equilibrium assumption for carbon is less certain. The diffusional growth of ferrite can be conceptualized as a two-step process occurring in series: carbon diffusion across the interface and subsequent carbon diffusion in austenite. At elevated temperatures, the high carbon diffusivity makes the first process negligible, and growth is primarily governed by the second step. However, as the temperature decreases, the carbon diffusivity decreases rapidly, and the carbon transfer across the interface may no longer be neglected and can lead to a carbon activity difference across the interface playing the role of a rate-limiting process [11,22]. This concept is consistent with the increasing experimental evidence of supersaturated bainite as the transformation temperature decreases. These supersaturation levels are not captured by the original Zener-Hillert theory, which is the second criticism raised against the diffusional theory.

Few attempts have addressed the potential formation of ferrite with a higher carbon content than allowed by local equilibrium. Hillert [11] presented a model where a carbon activity difference was assumed to exist across the ferrite/austenite interface. The carbon transfer from ferrite to austenite was expressed in terms of the carbon diffusion coefficient across the interface and the chemical potential difference across the interface. Hillert's qualitative calculations showed that the diffusional model can predict the occurrence of bainitic ferrite with supersaturated carbon content, if a carbon activity difference is allowed across the migrating interface Hillert's findings indicated increasing degree of supersaturation with decreasing nominal carbon content. A key limitation of this approach is that it does not permit a calculation of the chemical potential difference across the interface as a function of temperature. Another seminal contribution to understanding the carbon supersaturation in bainitic ferrite is due to Olson et al. [23,24] who argued that the transformation is controlled, simultaneously, by carbon partitioning and the movement of interfacial dislocations. This type of transformation has been referred to as a diffusional-displacive transformation. The calculations showed an increasing degree of supersaturation during the bainitic transformation with decreasing temperature and nominal carbon content [25]. Different assumptions are made in the two models as summarized by Olson et al. [23] including the interface mobility (neglected by Hillert), constant radius of curvature at the plate tip (considered by Olson et al. [23] and variable by Hillert), and the stored energy due to shape deformation accompanying ferritic bainite formation (unaddressed by Hillert). Recently, Dai et al. [26] extended the Zener-Hillert classical model and incorporated the solute drag dissipated energy arising from carbon diffusion across the interface to model the carbon supersaturation in bainite. The authors claim good agreement between the calculations and the measured carbon supersaturation.

Both Hillert's and Olson et al. models were subject to qualitative evaluation but were not tested against experimental data due to the absence of reliable experimental measurements of the carbon content in bainitic ferrite. However, the landscape has evolved significantly, with an increasing body of direct evidence showing bainite formation with carbon supersaturation [27–37]. Advances in atom probe tomography (APT) and in situ synchrotron X-ray diffraction have played a crucial role in providing fresh insights into carbon distribution within bainitic ferrite.

Caballero et al. took advantage of the slow transformation kinetics in nanocrystalline bainitic steels at low temperatures (~200 °C) to measure carbon content in bainitic laths using APT, revealing substantial carbon levels surpassing PE predictions [29]. In a complementary investigation, Caballero et al. [31] extended their analysis to other steels heat treated at different temperatures. The results further confirmed the presence of carbon in bainite in quantities surpassing the PE limits at temperatures below 350 °C. Recently, Pushkareva et al. [35] used APT, High-Energy X-ray Diffraction (HEXRD), and Electron Energy-Loss Spectroscopy in Transmission Electron Microscopy (EELS-TEM), to analyze the carbon content in carbide-free bainite. Results from all three techniques were consistent and confirmed the presence of high amounts of carbon in bainitic ferrite. It was also shown that carbon supersaturation increases with decreasing transformation temperature.

It is important to note that the quantification of carbon content using the abovementioned techniques is not perfect and includes various experimental uncertainties. X-ray techniques, relying on lattice parameter measurements, are affected not only by carbon content but also by factors like residual stresses, alloying elements, and potential bainite tetragonality [34,35,38]. These methods also average carbon content in bainitic ferrite, potentially including regions with carbon clusters, and thus affect the measured values. APT, despite its high spatial resolution, faces limitations due to the small volumes it analyzes, raising questions about statistical significance in quantitative measurements [34,35,39]. Nevertheless, the agreement across techniques and consistency in results across diverse steel chemistries provide convincing evidence of carbon supersaturation in bainitic ferrite. The data also consistently shows trends such as increased supersaturation as the transformation temperature decreases.

In the present study, the Zener-Hillert model, as previously modified by the present authors [19], is extended to account for the possible growth of bainitic ferrite with carbon supersaturation, by relaxing the constraint of carbon local equilibrium at the migrating interface, as previously suggested in other studies by Leach et al. [22] and Hillert [11]. The new version of the model will be introduced, used to predict the evolution of the carbon content in bainitic ferrite and then compared with the existing literature measurements of the carbon supersaturation in bainite.

To explain the extension to the Zener-Hillert model, we begin with the approach presented by Leach et al. [40]. Leach et al. assumes that the bainite growth kinetics are controlled by carbon diffusion in austenite. The maximum velocity of the ferritic plate, v_{max}, is calculated as:

$$v_{max} = \frac{D}{2\rho}\frac{x^{\gamma/\alpha} - x^0}{x^0 - x^{\alpha/\gamma}} \tag{1}$$

D is the carbon diffusivity in austenite and ρ is radius of curvature of the growing plate tip. $x^{\gamma/\alpha}$, and $x^{\alpha/\gamma}$ are the carbon mole fractions at the austenite and ferrite sides of the interface, respectively, and x^0 is the carbon mole fraction in the bulk. The carbon diffusion coefficient in austenite used in this study is from Ågren et al.'s work [41]. It is important to note that this coefficient was determined at temperatures exceeding the eutectoid temperature and is extrapolated to lower temperatures. It is not known how well this extrapolation reproduces the real carbon diffusivity at low temperatures. In the previous Eq. (1), the unknowns are the carbon content at both sides of the interface ($x^{\gamma/\alpha}$ and $x^{\alpha/\gamma}$), and the radius of curvature (ρ). To solve this problem, we need to consider 3 more independent equations.

The chemical driving force for growth is estimated using the expression proposed by Hillert et al. [42].:

$$\Delta G_m^{chem} = \sum^{X} u_X^{\gamma}\left(\mu_X^{\gamma,i} - \mu_X^{\alpha,i}\right) + u_{Fe}^{\gamma}\left(\mu_{Fe}^{\gamma,i} - \mu_{Fe}^{\alpha,i}\right) + u_C^{\gamma}\left(\mu_C^{\gamma,i} - \mu_C^{\alpha,i}\right) \tag{2}$$

where u is the U fractions ($u_i = \frac{x_i}{1-x_c}$) of Fe, X and C elements at the austenite and ferrite interface sides, and μ is the chemical potential. The U fractions of Fe and X elements are considered constant across the interface, which is equivalent to considering that substitutional elements are immobile. One should note that the above cited driving force represents the driving force for the interface migration as stated by Hillert, where the dissipated Gibbs energy portion due to carbon diffusion across the interface was subtracted from the full driving force [11]. In the recent study by Dai et al. [26], those authors considered the driving force for the entire process and then subtracted the solute drag force due to carbon diffusion across the interface.

Following Leach et al. [22] and Hillert [11], the carbon flux, J, across the interface can be expressed as:

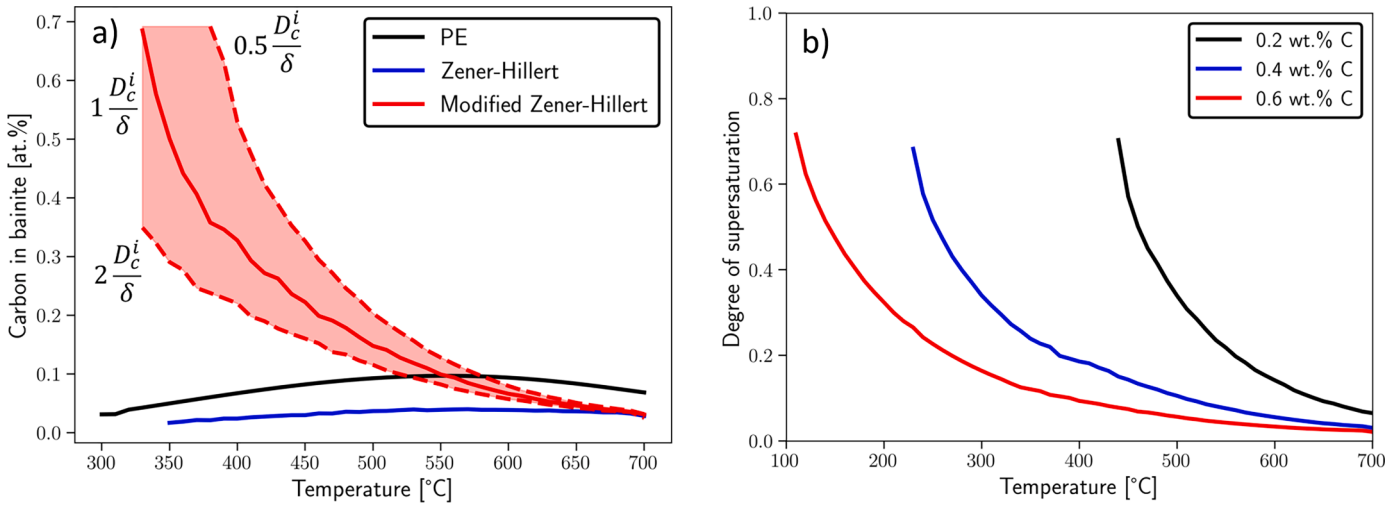

Fig. 1. a) Carbon content in ferrite for a 0.22C wt.% (1 at.%) steel (022CBF in Table 1) as function of temperature as predicted under PE conditions, the Zener-Hillert model without the present modifications and the same model with incorporating the modifications as detailed in the text. The red shaded area represents the estimated error on the predicted carbon content originating from the uncertainty on the fitting parameter, the upper and lower limits were calculated using a factor of 0.5 and 2 of the fitting parameter ($\frac{D_C^i}{\delta}$), b) Degree of carbon supersaturation ($\frac{Carbon\ in\ bainite}{Nominal\ carbon}$) in plate-like ferrite, as predicted by the present model, as a function of temperature, for different nominal carbon contents: 0.2 wt.% (black), 0.4 wt.% (blue) and 0.6 wt.% (red).

$$J_C^i = -L_C\frac{\partial\mu_C^i}{\partial x} = -\frac{L_C}{\delta}\left(\mu_C^{\gamma,i}-\mu_C^{\alpha,i}\right) = -\frac{1}{RTV_m}\frac{D_C^i\,x_C^i}{\delta}\left(\mu_C^{\gamma,i}-\mu_C^{\alpha,i}\right) \quad (3)$$

where R, T and V_m are the gas constant, temperature, and the molar volume of ferrite, respectively. For simplicity, a constant partial molar volume fraction was used for all components and phases. $\left(\mu_C^{\gamma,i}-\mu_C^{\alpha,i}\right)$ is the chemical potential difference across the interface. L_C is the cross interface diffusion parameter, which is equal to $\frac{D_C^i\,x_C^i}{RTV_m}$, where D_C^i is the carbon diffusion coefficient across the interface, δ is the interface width and $\frac{D_C^i}{\delta}$ is the carbon diffusion velocity across the interface. x_C^i is the mole fraction of carbon diffusing through the interface. This value was chosen here as the carbon content in ferrite side of the interface, $x_C^{\alpha/\gamma}$. D_C^i and δ, are not known with any certainty and cannot be easily determined experimentally. For the present study, D_C^i was set as D_C^γ, the carbon diffusivity in austenite and δ as 0.25 nm. One can regard the $\frac{D_C^i}{\delta}$ as the fitting parameter of the present study.

Under steady state conditions and using the flux balance for carbon, one can write:

$$\mu_C^{\gamma,i}-\mu_C^{\alpha,i} = -\frac{\delta\,RT}{D_C^i\,x_C^i}\,v_{max}\left(x^{\gamma/\alpha}-x^{\alpha/\gamma}\right) \quad (4)$$

In the classic Zener-Hillert model, local equilibrium is assumed for carbon across the interface and thus the term on the left of Eq. (4) is zero. This assumption is relaxed in the present extended model and the new formalism allows ferrite to grow with partial supersaturation if a difference in carbon activity exists across the interface.

The available energy (Eq. (2)) is balanced by the energy dissipated due to solute diffusion across the interface, ΔG_m^{SD}, the energy dissipated against friction, ΔG_m^{fric}, the interface curvature, ΔG_m^{r} and the interaction between the interface and the present obstacles in austenite, ΔG_m^{mec}.

$$\Delta G_m^{chem} = \Delta G_m^{r} + \Delta G_m^{mec} + \Delta G_m^{SD} + \Delta G_m^{fric} \quad (5)$$

Both ΔG_m^{SD} and ΔG_m^{fric} were neglected in the current calculations due to the high velocities observed at such low temperatures for bainite formation, as well as the high mobility for such interfaces as reported by Hillert [11,26]. $\Delta G_m^{r} = V_m\frac{\sigma^{\gamma/\alpha}}{\rho}$, $\sigma^{\gamma/\alpha}$ is the interfacial energy (set to 0.23 J. m^{-2} [13]), $\Delta G_m^{mec} = \hat{\sigma}\frac{b}{\Lambda}m_s$, $\hat{\sigma}$ (the internal back stress) represents the opposing force generated by the defects (such as dislocations and solute atoms), m_s is the Schmid factor, b is the magnitude of the Burgers vector, and Λ is the mean spacing between disconnections [19].

Table 1
Chemical compositions (in wt.%) of the steels used for comparison with the calculations.

	C	Mn	Si	Mo	Cr	Al	Ni	V
MC-LSi	0.3	1.22	0.25	0.03	0.14	–	0.1	–
MC—HSi	0.29	2.06	1.48	0.27	0.43	–	–	–
HC—HSi	0.98	1.89	1.46	0.26	1.26	–	–	–
022CBF	0.22	2.2	1.8	0.2	–	0.01	–	–
Alloy1	1	1.9	1.5	0.26	1.3	–	–	0.1
Alloy2	0.7	1.3	1.4	0.24	1.0	–	0.1	–

Eqs. (1), (4) and (5) can be used to calculate the growth velocity for a given alloy composition, temperature, and interface curvature, ρ. Thermodynamic quantities are calculated using the TCFE9 database of Thermo-Calc [43], and following Zener, we assume that the conditions leading to the maximum velocity dominate [11,15]. To this end, velocities are computed at different radii of curvature, and the curvature corresponding to the maximum velocity is selected as the operating curvature. A flowchart describing the calculation procedure is given in Fig.S1 of the supplementary materials.

Fig. 1-a compares the expected carbon content in bainitic ferrite as a function of temperature, as calculated under PE conditions, the original Zener-Hillert model, and the current model. The calculations were performed for a steel with a 0.22 wt.% carbon content (022CBF in Table 1).

At temperatures exceeding ~ 600 °C, both the Zener-Hillert model and the present model predict ferrite formation with a local equilibrium carbon content, lower than PE values. This is due to interface curvature and barrier energy effects (Eq. (5)). As the temperature decreases, the original Zener-Hillert model predicts that the carbon content in ferrite follows a similar trend to the PE predictions, albeit to a lower extent. In original Zener-Hillert model, low-temperature ferrite is not expected to exhibit any significant carbon supersaturation. In contrast, the modified model predicts increasing carbon concentration in bainitic ferrite as temperature decreases, especially below 500 °C, indicating significant supersaturation. The results shown in Fig. 1-a illustrate the sensitivity of carbon supersaturation evolution to variations in the cross-boundary

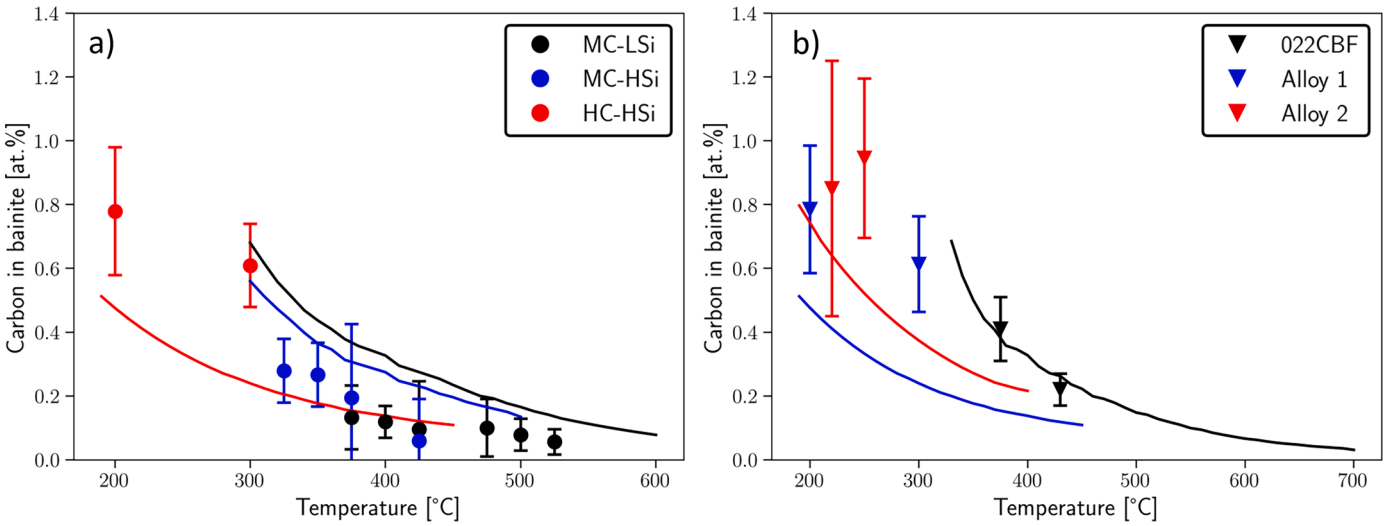

Fig. 2. Comparison between carbon content in bainite as measured experimentally (dots) and the predicted ones using the present model (solid lines).

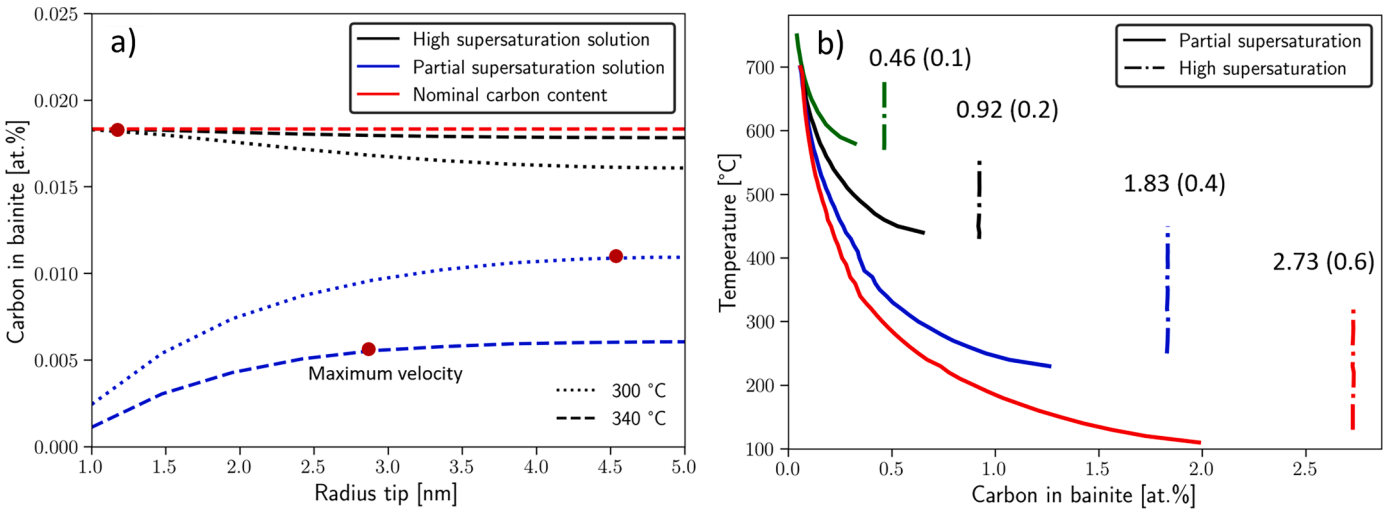

Fig. 3. a) Carbon content in bainite as calculated using the present model for a Fe-0.4C wt.% (1.83 at.%) alloy at 300 °C and 340 °C. The blue curve represents the partial supersaturation solution, and the black curve is the high supersaturation solutions. The nominal content is shown in red. b) Carbon content in bainite as a function of temperature considering the two solutions as shown in Fig. 3-a. The left-hand lines correspond to the partial supersaturation solution selected using the maximum velocity criterion, and the right-hand lines correspond to the high supersaturation solution. The colors denote different nominal carbon contents, expressed in at.% (wt.%), in proximity to each curve.

diffusion coefficient. The temperature and concentration dependencies of this coefficient across the interface remain unknown. In this study, and for simplicity, we hypothesize that these dependencies equal those of carbon diffusion coefficient within austenite.

The effect of bulk alloy carbon content on the degree of carbon supersaturation $\left(\frac{Carbon\ in\ bainite}{Nominal\ carbon}\right)$ in the plate-shaped ferrite is shown in Fig. 1-b for various nominal bulk carbon contents. The degree of supersaturation increases as the nominal carbon content decreases. This is consistent with the reports of Mujahid et al. [25] (using the model developed by Olson et al. [23]) as well as Hillert [11].

A comparison of the model predictions with the experimentally measured carbon contents in bainitic ferrite is shown in Fig. 2-a and Fig. 2-b The chemical compositions of the steels used for this comparison are listed in Table 1. The experimental measurements reported in Fig. 2 were all carried out using APT.

The model reproduces well the experimental trend, showing increasing carbon supersaturation in the bainitic ferrite with decreasing temperature. The model seems to capture both the effect of temperature and alloy composition, considering the diverse experimental data covering varying temperatures, low and high carbon contents, and different substitutional alloying additions (Table 1). However, some differences are present between the absolute values of the measured carbon content in bainite and those predicted by the model. The limitations of atom probe tomography (APT) in analyzing small volumes warrant careful interpretation of measured carbon content. At the same time the model predictions are affected by the uncertain choice of the cross-boundary diffusion coefficient. The results, however, suggest that bainite containing a supersaturation of carbon can be described within the framework of the diffusional theory, when a carbon activity difference at the austenite/ferrite interface exists due to the need to consider the sequential nature of both the carbon diffusion across the interface, and the diffusion in the austenite, at low temperatures.

It is very interesting to observe that below the M_s temperature, the model calculations indicate that, for a given tip radius, ferrite plates can grow either with a partial supersaturation or with a very high supersaturation nearing the nominal bulk content. This bifurcation behavior is shown in Fig. 3-a for a Fe-0.4C (wt.%) alloy at 300 °C and 340 °C

($M_s \sim 370$ °C [44]). In this case, the calculations illustrate two possible solutions for the set of Eqs. (1), (4) and (5). For the partial supersaturation solution, the carbon content in bainitic ferrite increases with the tip radius, reaching a maximum at approximately $\rho = 3 - 4$ *nm*, and then gradually decreases with an increase in curvature radius. For the high supersaturation solution, the carbon content in bainite shows values close to the bulk content and decreases gradually with an increasing radius of curvature.

Using Zener's maximum growth rate hypothesis, which selects the radius of curvature that yields the maximum velocity, the carbon content in bainite was estimated from both solutions and plotted as a function of temperature in Fig. 3-b for various Fe-C alloys. The solid lines correspond to partial carbon supersaturation solutions and are similar to those shown in Fig. 1-a. The dot-dash lines correspond to the high carbon supersaturation solution, showing an asymptotic line in proximity to the nominal carbon content. The high supersaturation solution is only present over a specific temperature range, as shown by the calculations. For example, for the Fe-0.4C wt.%, the high supersaturation solution is observed from 470 °C down to 300 °C (Ms ~ 370 °C). Below 300 °C, neither solution is viable, and bainite growth is impossible in this case.

The two solutions shown in Fig. 3-b align with Hillert's earlier findings of bifurcation behavior as carbon content decreases [6,11]. Hillert attributed the high supersaturation solution to the martensitic transformation. Specifically, he proposed that a ferrite lath initially growing with a small tip radius would first exhibit partial supersaturation, but potentially transitioning to martensite if the tip radius increases. One might argue that the second solution shows the possibility for bainite to grow under conditions where growth is interface controlled, and no long-range carbon diffusion occurs during the growth of the plates. It is interesting that two distinct solutions exist as this would suggest the presence of two different transformation products one being bainite and the other being martensite. One might even suggest that the above model, showing a change in supersaturation with decreasing temperature due to the increasing importance of the time required for carbon diffusion across the migrating interface, provides a means of reconciling the age-old debate between the diffusional and diffusionless models of bainite formation.

Bainite forming below Ms, as shown in Fig. 3-b, aligns with experimental observations where both bainite and martensite are observed at temperatures below Ms [45–48]. The formation of bainite at these temperatures has not been well-described by diffusional models in the past due to the very slow kinetics predicted by the classic Zener-Hillert model [47]. The experimental data can be accurately described, however, if the constraint of maintaining carbon equilibrium across the interface is relaxed, as would be expected at such low temperatures. At low temperatures and, consequently increasing supersaturation levels, the carbon content in ferrite approaches the bulk carbon content, and the velocity tends to increase (Eq. 1), compensating for the low diffusivity of carbon in austenite.

In summary, the carbon supersaturation observed in bainite formed at low temperatures can be captured by relaxing the assumption of carbon local equilibrium in the Zener-Hillert model. Carbon local equilibrium will be expected at high temperatures, due to the high carbon diffusivity, but as the transformation temperature decreases this becomes less likely. The resulting carbon activity difference across the interface leads to the formation of bainite with carbon supersaturation. The comparison between the experimentally reported and the predicted carbon contents in bainitic ferrite using the modified Zener-Hillert theory show good agreement, providing, for the first time, a semi-quantitative estimate of the carbon content in bainite.

To advance this analysis, the present model should be tested to simultaneously predict the lengthening kinetics of bainitic ferrite and the carbon content in both austenite and bainitic ferrite for the same alloy at different temperatures. Existing experimental data are limited to either growth kinetics or carbon content measurements for a given alloy. Future experimental efforts could focus on conducting measurements of growth kinetics for the same alloys studied in this paper, addressing this gap within the literature.

CRediT authorship contribution statement

Imed-Eddine Benrabah: Writing – review & editing, Writing – original draft, Methodology, Investigation, Formal analysis, Data curation. **Yves Brechet:** Writing – review & editing, Formal analysis, Conceptualization. **Christopher Hutchinson:** Writing – review & editing, Formal analysis, Conceptualization. **Hatem Zurob:** Writing – review & editing, Supervision, Funding acquisition, Formal analysis, Conceptualization.

Declaration of competing interest

The authors declare that they have no known competing financial interests or personal relationships that could have appeared to influence the work reported in this paper.

Acknowledgements

HZ acknowledges the support of the Natural Science and Engineering Research Council of Canada.

Supplementary materials

Supplementary material associated with this article can be found, in the online version, at doi:10.1016/j.scriptamat.2024.116182.

References

[1] R.F. Hehemann, K.R. Kinsman, H.I. Aaronson, A debate on the bainite reaction, Metall. Trans. 3 (1972) 1077–1094, https://doi.org/10.1007/BF02642439.
[2] H.I. Aaronson, M.G. Hall, A History of the Controversy over the Roles of Shear and Diffusion in Plate Formation above Ma and a Comparison of the Atomic Mechanisms of These Processes, Metall. Mater. Trans. A 25 (1994) 1797–1819.
[3] H.K.D.H. Bhadeshia, Bainite in steels: transformations, Microstructure and Properties, 2. ed, IOM Communications, London, 2001.
[4] H.K.D.H. Bhadeshia, Bainite: overall transformation kinetics, J. Phys. Colloques 43 (1982), https://doi.org/10.1051/jphyscol:1982468. C4-443-C4-448.
[5] H.K.D.H. Bhadeshia, D.V. Edmonds, The mechanism of bainite formation in steels, Acta Metall. 28 (1980) 1265–1273, https://doi.org/10.1016/0001-6160(80)90082-6.
[6] G.R. Purdy, M. Hillert, Overview no. 38: on the nature of the bainite transformation in steels, Acta Metall. 32 (1984) 823–828, https://doi.org/10.1016/0001-6160(84)90018-X.
[7] G.I. Rees, H.K.D.H. Bhadeshia, Bainite transformation kinetics Part 1 Modified model, Mater. Sci. Technol. 8 (1992) 985–993, https://doi.org/10.1179/mst.1992.8.11.985.
[8] A. Borgenstam, M. Hillert, J. Ågren, Metallographic evidence of carbon diffusion in the growth of bainite, Acta Mater. 57 (2009) 3242–3252, https://doi.org/10.1016/j.actamat.2009.03.026.
[9] M. Hillert, Diffusion in growth of bainite, Metall. Mater. Trans. A 25 (1994) 1957–1966, https://doi.org/10.1007/BF02649044.
[10] M. Hillert, The nature of bainite, ISIJ Int. 35 (1995) 1134–1140, https://doi.org/10.2355/isijinternational.35.1134.
[11] M. Hillert, The growth of ferrite, bainite and martensite, Report, Swedish Inst. Metal Res. Stockholm (1960) 113–158.
[12] M. Hillert, L. Höglund, J. Ågren, Role of carbon and alloying elements in the formation of bainitic ferrite, Metall. Mat. Trans A 35 (2004) 3693–3700, https://doi.org/10.1007/s11661-004-0275-5.
[13] L. Leach, M. Hillert, A. Borgenstam, Modeling C-Curves for the growth rate of widmanstätten and bainitic ferrite in Fe-C alloys, Metall. Mater. Trans. A 47 (2016) 19–25, https://doi.org/10.1007/s11661-015-3241-5.
[14] M.J. Santofimia, F.G. Caballero, C. Capdevila, C. García-Mateo, C.G. de Andrés, New model for the overall transformation kinetics of bainite. part 1: the model, Mater. Trans. 47 (2006) 2465–2472, https://doi.org/10.2320/matertrans.47.2465.
[15] J. Yin, L. Leach, M. Hillert, A. Borgenstam, C-Curves for lengthening of widmanstätten and bainitic ferrite, Metall. Mater. Trans. A 48 (2017) 3997–4005, https://doi.org/10.1007/s11661-017-4196-5.
[16] D. Quidort, Y.J.M. Brechet, A model of isothermal and non isothermal transformation kinetics of bainite in 0.5% C steels, ISIJ Int. 42 (2002) 1010–1017, https://doi.org/10.2355/isijinternational.42.1010.
[17] D. Quidort, Y. Bréchet, The role of carbon on the kinetics of bainite transformation in steels, Scr. Mater. 47 (2002) 151–156, https://doi.org/10.1016/S1359-6462(02)00121-5.

[18] H.K.D.H. Bhadeshia, The bainite transformation: unresolved issues, Mat. Sci. Eng.: A 273–275 (1999) 58–66, https://doi.org/10.1016/S0921-5093(99)00289-0.
[19] I.-E. Benrabah, Y. Brechet, G. Purdy, C. Hutchinson, H. Zurob, On the origin of the barrier in the bainite phase transformation, Scr. Mater. 223 (2023) 115076, https://doi.org/10.1016/j.scriptamat.2022.115076.
[20] A. Phillion, H.W. Zurob, C.R. Hutchinson, H. Guo, D.V. Malakhov, J. Nakano, G. R. Purdy, Studies of the influence of alloying elements on the growth of ferrite from austenite under decarburization conditions: fe-C-Nl alloys, Metall. Mater. Trans. A 35 (2004) 1237–1242, https://doi.org/10.1007/s11661-004-0297-z.
[21] A. Béché, H.S. Zurob, C.R. Hutchinson, Quantifying the Solute Drag Effect of Cr on Ferrite Growth Using Controlled Decarburization Experiments, Metall. Mater. Trans. A 38 (2007) 2950–2955. https://doi.org/10.1007/s11661-007-9353-9.
[22] L. Leach, J. Ågren, L. Höglund, A. Borgenstam, Diffusion-Controlled Lengthening Rates of Bainitic Ferrite a Part of the Steel Genome, Metall. Mater. Trans. A 50 (2019) 2613–2618, https://doi.org/10.1007/s11661-019-05208-x.
[23] G.B. Olson, H.K.D.H. Bhadeshia, M. Cohen, Coupled diffusional/displacive transformations, Acta Metall. 37 (1989) 381–390, https://doi.org/10.1016/0001-6160(89)90222-8.
[24] G.B. Olson, H.K.D.H. Bhadeshia, M. Cohen, Coupled diffusional/displacive transformations: part II. Solute trapping, Metall. Trans. A 21 (1990) 805–809, https://doi.org/10.1007/BF02656563.
[25] S.A. Mujahid, H.K.D.H. Bhadeshia, Coupled diffusional/displacive transformations: effect of carbon concentration, Acta Metall. Mater. 41 (1993) 967–973, https://doi.org/10.1016/0956-7151(93)90031-M.
[26] Z. Dai, H. Chen, J. Sun, S. van der Zwaag, J. Sun, Carbon solute drag effect on the growth of carbon supersaturated bainitic ferrite: modeling and experimental validations, Acta Mater. (2024) 119791, https://doi.org/10.1016/j.actamat.2024.119791.
[27] F. Caballero, M. Miller, S. Babu, C. Garciamateo, Atomic scale observations of bainite transformation in a high carbon high silicon steel, Acta Mater. 55 (2007) 381–390, https://doi.org/10.1016/j.actamat.2006.08.033.
[28] F.G. Caballero, M.K. Miller, A.J. Clarke, C. Garcia-Mateo, Examination of carbon partitioning into austenite during tempering of bainite, Scr. Mater. 63 (2010) 442–445, https://doi.org/10.1016/j.scriptamat.2010.04.049.
[29] F.G. Caballero, M.K. Miller, C. Garcia-Mateo, Carbon supersaturation of ferrite in a nanocrystalline bainitic steel, Acta Mater. 58 (2010) 2338–2343, https://doi.org/10.1016/j.actamat.2009.12.020.
[30] F.G. Caballero, M.K. Miller, C. García-Mateo, Slow Bainite: an opportunity to determine the carbon content of the bainitic ferrite during growth, SSP 172–174 (2011) 111–116, https://doi.org/10.4028/www.scientific.net/SSP.172-174.111.
[31] F.G. Caballero, M.K. Miller, C. Garcia-Mateo, J. Cornide, M.J. Santofimia, Temperature dependence of carbon supersaturation of ferrite in bainitic steels, Scr. Mater. 67 (2012) 846–849, https://doi.org/10.1016/j.scriptamat.2012.08.007.
[32] C. Garcia-Mateo, J.A. Jimenez, H.-W. Yen, M.K. Miller, L. Morales-Rivas, M. Kuntz, S.P. Ringer, J.-R. Yang, F.G. Caballero, Low temperature bainitic ferrite: evidence of carbon super-saturation and tetragonality, Acta Mater. 91 (2015) 162–173, https://doi.org/10.1016/j.actamat.2015.03.018.
[33] R. Rementeria, J.D. Poplawsky, M.M. Aranda, W. Guo, J.A. Jimenez, C. Garcia-Mateo, F.G. Caballero, Carbon concentration measurements by atom probe tomography in the ferritic phase of high-silicon steels, Acta Mater. 125 (2017) 359–368, https://doi.org/10.1016/j.actamat.2016.12.013.
[34] R. Rementeria, J.A. Jimenez, S.Y.P. Allain, G. Geandier, J.D. Poplawsky, W. Guo, E. Urones-Garrote, C. Garcia-Mateo, F.G. Caballero, Quantitative assessment of carbon allocation anomalies in low temperature bainite, Acta Mater. 133 (2017) 333–345, https://doi.org/10.1016/j.actamat.2017.05.048.
[35] I. Pushkareva, J. Macchi, B. Shalchi-Amirkhiz, F. Fazeli, G. Geandier, F. Danoix, J. D.C. Teixeira, S.Y.P. Allain, C. Scott, A study of the carbon distribution in bainitic ferrite, Scr. Mater. 224 (2023) 115140, https://doi.org/10.1016/j.scriptamat.2022.115140.
[36] C. Rampelberg, S.Y.P. Allain, G. Geandier, J. Teixeira, F. Lebel, T. Sourmail, Carbide-Free bainite transformations above and below martensite start temperature investigated by in-situ high-energy X-Ray diffraction, JOM 73 (2021) 3181–3194, https://doi.org/10.1007/s11837-021-04903-8.
[37] S. Gaudez, J. Teixeira, S. Denis, G. Geandier, S.Y.P. Allain, Martensite and nanobainite transformations in a low alloyed steel studied by in situ high energy synchrotron diffraction, Mater. Charact. 185 (2022) 111740, https://doi.org/10.1016/j.matchar.2022.111740.
[38] H.K.D.H. Bhadeshia, Anomalies in carbon concentration determinations from nanostructured bainite, Mater. Sci. Technol. 31 (2015) 758–763, https://doi.org/10.1179/1743284714Y.0000000655.
[39] R. Rementeria, C. Capdevila, R. Domínguez-Reyes, J.D. Poplawsky, W. Guo, E. Urones-Garrote, C. Garcia-Mateo, F.G. Caballero, Carbon Clustering in Low-Temperature Bainite, Metall. Mat. Trans. A 49 (2018) 5277–5287, https://doi.org/10.1007/s11661-018-4899-2.
[40] M. Hillert, The role of interfacial energy during solid-state phase transformations, Jernkontorets Annaler 141 (1957) 757–789.
[41] J. Ågren, A revised expression for the diffusivity of carbon in binary Fe-C austenite, Scr. Metall. 20 (1986) 1507–1510, https://doi.org/10.1016/0036-9748(86)90384-4.
[42] M. Hillert, Solute drag, solute trapping and diffusional dissipation of Gibbs energy1, Acta. Mater. 47 (1999) 4481–4505, https://doi.org/10.1016/S1359-6454(99)00336-5.
[43] J.-O. Andersson, T. Helander, L. Höglund, P. Shi, B. Sundman, Thermo-Calc & DICTRA, computational tools for materials science, Calphad 26 (2002) 273–312.
[44] S.M.C. van Bohemen, Bainite and martensite start temperature calculated with exponential carbon dependence, Mater. Sci. Technol. 28 (2012) 487–495, https://doi.org/10.1179/1743284711Y.0000000097.
[45] P. Kolmskog, A. Borgenstam, M. Hillert, P. Hedström, S.S. Babu, H. Terasaki, Y.-I. Komizo, Direct observation that bainite can grow below MS, Metall. Mater. Trans. A 43 (2012) 4984–4988, https://doi.org/10.1007/s11661-012-1342-y.
[46] S.M.C. van Bohemen, M.J. Santofimia, J. Sietsma, Experimental evidence for bainite formation below Ms in Fe–0.66C, Scr. Mater. 58 (2008) 488–491, https://doi.org/10.1016/j.scriptamat.2007.10.045.
[47] S. Samanta, P. Biswas, S. Giri, S.B. Singh, S. Kundu, Formation of bainite below the MS temperature: kinetics and crystallography, Acta Mater. 105 (2016) 390–403, https://doi.org/10.1016/j.actamat.2015.12.027.
[48] N.N. Thadhani, M.A. Meyers, Kinetics of isothermal martensitic transformation, Prog. Mater Sci. 30 (1986) 1–37, https://doi.org/10.1016/0079-6425(86)90002-2.